Phase sensitive electron-phonon coupling in a superconducting proximity structure

T. T. Heikkilä*
Low Temperature Laboratory, Helsinki University of Technology, P.O. Box 5100, FIN-02015 TKK, Espoo, Finland

Francesco Giazotto
NEST CNR-INFM and Scuola Normale Superiore, I-56126 Pisa, Italy

(Received 27 October 2008; revised manuscript received 30 January 2009; published 11 March 2009)

We study the role of the superconducting proximity effect on the electron-phonon energy exchange in diffusive normal metals (N) attached to superconductors (S). The proximity effect modifies the spectral response of the normal metal, in particular the local density of states. This leads to a weakening of the electron-phonon energy relaxation. We show that the effect is easily observable with modern thermometry methods and predict that it can be tuned in structures connected to multiple superconductors by adjusting the phase difference between superconducting order parameters at the two NS interfaces.

DOI: 10.1103/PhysRevB.79.094514 PACS number(s): 72.10.−d, 72.15.Eb, 74.25.Kc, 74.45.+c

I. INTRODUCTION

The state of an electron system subject to driving depends on three ingredients: on the external driving, on the response functions of the system, and on internal and external relaxations within the system and out of the system. For sufficiently strong but constant driving, the system can be brought out of equilibrium from its surroundings, in which case the steady state can be determined from a balance between the driving and the relaxation. By far, the most relevant relaxation mechanism for electrons in metals is caused by the coupling between electrons and phonons. If the dominant relaxation mechanism is known to a high accuracy, the result of such heat balance can be used to study the driving. An example of such a procedure takes place in hot-electron thermal radiation detectors,[1,2] which rely on the changes in the electron temperature due to changes in the amount of radiation coupling to the device and driving the electron system. Typically such devices require accurate thermometry through an easily measurable observable that is sensitive to the electron temperature. One such frequently employed thermometer is based on a junction between normal metals (N) and superconductors (S).

When a normal metal is brought in contact with superconductors, the superconducting order parameter leaks out to the normal side. This superconducting proximity effect[3] changes the spectral response of the system[4] but it also affects the relaxation mechanisms. In this paper we study how this effect manifests itself in the electron-phonon coupling and consider the schematic structure shown in Fig. 1. Some of the features induced by the proximity effect are the changes in the local density of states[5] and a finite pair amplitude inside the normal metal. For example, the density of states obtains a minigap whose size $E_g(\phi)$ depends on the phase difference ϕ between the superconductors,[6] at $\phi=0$ for $E_{\mathrm{Th}} \ll \Delta$, $E_g \approx 3.12E_{\mathrm{Th}}$ whereas $E_g=0$ at $\phi=\pi$. Here $E_{\mathrm{Th}}=\hbar D/L^2$ is the Thouless energy of the normal-metal piece with a diffusion constant D and length L and Δ is the energy gap of the superconductor.

By utilizing quasiclassical equations, we show how the collision integrals describing the electron-phonon coupling are changed by the proximity effect. We consider in particular the resulting effects on the electron-phonon relaxation rate and the heat power flowing between the two systems. Our examples are calculated for a SNS system where the normal metal is sandwiched between two superconductors. In this case the proximity-induced effects can also be tuned by adjusting the phase difference between the order parameters of the two superconducting contacts.

This paper is organized as follows. At first we derive the general diffusive-limit electron-phonon collision integrals from Usadel equation[7] for the Keldysh Green's functions.[8] Then we study especially the case when the electron system can be described with Fermi function at a local temperature T_e and the phonon system with Bose function at temperature T_p. For small deviations $|T_e-T_p| \ll T_e$ the collisions can be described with a relaxation rate, whose dependence on energy, temperature, and ϕ are shown for an example geometry. Then we concentrate on the energy current between the two systems, the quantity entering heat balance equations. This quantity is well defined for arbitrary temperature differences between the electron and phonon systems. Its depen-

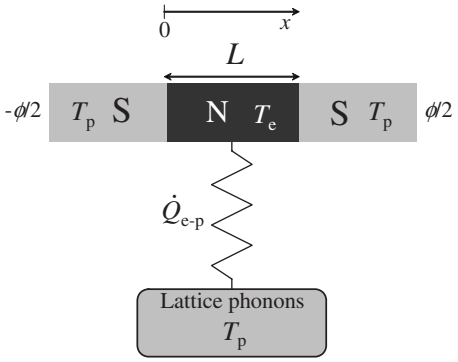

FIG. 1. Schematic structure considered in this paper: the superconducting electrodes (assumed to be large and residing at the phonon temperature T_p) induce a proximity effect into the normal metal. This proximity effect changes the spectrum of the electronic excitations and thereby also the electron-phonon energy exchange $\dot{Q}_{\mathrm{e\text{-}p}}$. The spectrum can be controlled via the phase difference ϕ of the superconducting order parameter. This allows one to explore the effect as shown below in Fig. 6.

dence on position, length of the normal metal, and ϕ are exemplified for example geometries. Finally we suggest how the phase dependence can be measured in a system easily manufactured with present experimental techniques.

II. THEORETICAL FRAMEWORK

When describing nonequilibrium superconductivity, it is convenient to concentrate separately on two types of excitations:[9] "longitudinal," described by the antisymmetric part $f_L=f(-E)-f(E)$ of the electron energy distribution function with respect to the chemical potential of the superconductor, and "transverse," described by the symmetric part $f_T=1-f(E)-f(-E)$. The previous describes "thermal" excitations whereas the latter is relevant for charged excitations. The detailed forms of the collision integrals for the two types of excitations are derived in the Appendix. At quasiequilibrium described by an effective temperature T_e, the most relevant type of excitations are the longitudinal ones. In this case, assuming that the elastic mean-free path exceeds the phonon wavelength,[1] the collision integral is given by

$$I_L = \lambda \int d\omega \omega^2 \, \mathrm{sgn}(\omega) K(\epsilon,\omega) R(\epsilon,\omega;T_e,T_p). \tag{1}$$

Here λ is the electron-phonon coupling constant, the kernel

$$K(\epsilon,\omega) = N(\epsilon)N(\epsilon+\omega) - F_c(\epsilon)F_c(\epsilon+\omega) - F_s(\epsilon)F_s(\epsilon+\omega)$$

describes the changes in the spectrum of the junction, $N(\epsilon)$ is the (local) reduced density of states, and $F_c(\epsilon)$ and $F_s(\epsilon)$ are projections of the pair amplitude (anomalous function) as described in Eq. (A1). The part depending on the phonon and electron temperatures is in quasiequilibrium,

$$R(\epsilon,\omega;T_e,T_p) = \tanh\left(\frac{\epsilon}{2k_BT_e}\right)\tanh\left(\frac{\epsilon+\omega}{2k_BT_e}\right) + \coth\left(\frac{\omega}{2k_BT_p}\right) \times\left[\tanh\left(\frac{\epsilon+\omega}{2k_BT_e}\right) - \tanh\left(\frac{\epsilon}{2k_BT_e}\right)\right] - 1.$$

The kernel $K(\epsilon,\omega)$ is in general position dependent, and thereby it makes also the collision integral depend on the position. Once this collision integral is known, it can be inserted in a kinetic equation, such as those presented in Ref. 4.

In what follows, we describe the electron-phonon scattering inside the SNS junction in terms of the scattering rate and the heat current flowing between the electron and phonon systems. In order to find the density of states and the anomalous function inside the normal region of the SNS junction, we solve numerically the Usadel equation[4,7,10,11]

$$D\nabla\cdot(\hat{g}^R\nabla\hat{g}^R) = [-i(\epsilon+i\gamma)\hat{\tau}_3,\hat{g}^R], \tag{2}$$

where γ is a small positive parameter describing inelastic scattering and the retarded Green's function $\hat{g}^R$ satisfies the normalization condition $(\hat{g}^R)^2=\hat{1}$. We assume that the NS interfaces are clean and that $\hat{g}^R$ obtains the form of the bulk Green's function $\hat{g}^R_{\mathrm{bulk}}=\epsilon_+/\sqrt{\epsilon_+^2-\Delta^2}\hat{\tau}_3+\Delta/\sqrt{\epsilon_+^2-\Delta^2}[\cos(\phi)i\hat{\tau}_2+\sin(\phi)i\hat{\tau}_1]$ at these boundaries. Here $\epsilon_+=\epsilon+i\gamma$, Δ is the absolute value of the superconducting order parameter, ϕ is its phase, and $\hat{\tau}_i$ are the Pauli matrices in Nambu space. For lower-transparency junctions the proximity effect and thereby the effects described below will be reduced.[10]

III. SCATTERING RATE

Close to equilibrium, the electron-phonon scattering can be described with an energy-dependent scattering rate.[12] The latter can be obtained by assuming that the Keldysh part of the scattering self-energy is related to the retarded (R) and advanced (A) parts via $\hat{\Sigma}^K=(\hat{\Sigma}^R-\hat{\Sigma}^A)f_L$ and similarly for the Green's function, $\hat{g}^K\approx(\hat{g}^R-\hat{g}^A)(f_L+\delta f_L)$. This gives us $I_L\approx\Gamma_{\mathrm{e\text{-}p}}^{\mathrm{SNS}}\delta f_L$ with

$$\Gamma_{\mathrm{e\text{-}p}}^{\mathrm{SNS}} = \frac{1}{2}\mathrm{Tr}[(\hat{g}^R-\hat{g}^A)(\hat{\Sigma}^R-\hat{\Sigma}^A)] = \lambda\int d\omega\omega^2\,\mathrm{sgn}(\omega)K(\epsilon,\omega)\frac{\cosh\left(\frac{\epsilon}{2k_BT}\right)}{\sinh\left(\frac{\omega}{2k_BT}\right)\cosh\left(\frac{\epsilon+\omega}{2k_BT}\right)}. \tag{3}$$

In the absence of superconductivity, $N(\epsilon)\approx 1$ is approximately a constant and $F_c=F_s\equiv 0$. In this case at $\epsilon=0$ we get $\Gamma_{\mathrm{e\text{-}p}}^N=7\lambda\zeta(3)(k_BT)^3$.[13]

The scattering rate is plotted in Fig. 2 as a function of energy for a few phases ϕ and at two different temperatures. The plotted rate is averaged across the weak link,

$$\Gamma_{\mathrm{e\text{-}p}} = \frac{1}{L}\int_0^L dx\Gamma_{\mathrm{e\text{-}p}}^{\mathrm{SNS}}(x),$$

and normalized to $\Gamma_{\mathrm{e\text{-}p}}^N$ to illustrate the corrections due to the proximity effect. At energies $\epsilon>k_BT$ the rate rises as ϵ^3 in the absence of superconductivity. The main modification due to the proximity effect is the phase-dependent minigap, which causes a huge drop in the scattering rates. Moreover, above the minigap the rates are slightly lower than in the absence of the proximity effect—this is due to the fact that within a thermal coherence length $\xi_T=\sqrt{\hbar D/(2\pi k_BT)}$ from the NS interfaces electron-phonon coupling is weakened at any value of the phase (see Fig. 3).

IV. HEAT CURRENT

The most relevant quantity in describing the electron-phonon interaction is the heat current associated with a temperature difference in the electron and phonon systems. This quantity can be described also far from equilibrium, i.e., for arbitrary difference between the electron and phonon temperatures. The heat current density is obtained by multiplying I_L with energy ϵ and the normal-state density of states ν_F at the Fermi energy and integrating over the energy

$$P_{\mathrm{e\text{-}p}} = \lambda\nu_F\int d\epsilon d\omega\epsilon\omega^2\,\mathrm{sgn}(\omega)K(\epsilon,\omega)R(\epsilon,\omega;T_e,T_p). \tag{4}$$

In the normal state, the integral can be evaluated analytically, with the result[14]

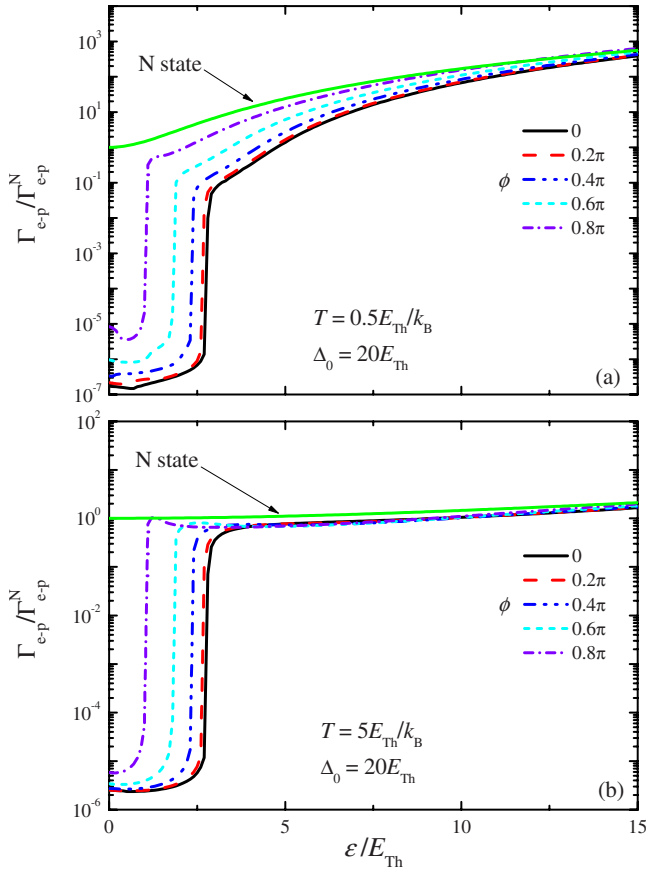

FIG. 2. (Color online) Phase and energy dependences of the electron-phonon scattering rate $\Gamma_{e\text{-}p}$ normalized to the normal-state zero-energy result $\Gamma^N_{e\text{-}p}=7\lambda\zeta(3)(k_BT)^3$ at two different temperatures (top: $k_BT=E_{Th}/2$; bottom: $k_BT=5E_{Th}$). We have assumed $\Delta_0=20E_{Th}$ and averaged the rates across the normal-metal piece. The solid line shows the energy dependence obtained in the normal case for which $K(\epsilon,\omega)=1$. Note the logarithmic scale of the figure. The exact low-energy values in the presence of the proximity effect depend on the magnitude of the inelastic-scattering parameter γ in Eq. (2). Here and throughout we have chosen $\gamma=10^{-5}E_{Th}$.

$$P^N_{e\text{-}p} = \Sigma\,(T_p^5 - T_e^5), \tag{5}$$

where $\Sigma=24\zeta(5)\nu_F k_B^5\lambda$. Measured values of Σ in different metals are tabulated in Ref. 1.

In most cases, the heat diffusion within the normal metal is much stronger than out from it. In this case the variations in the temperature of the normal metal become small and the average temperature is determined by the rate integrated over the volume of the junction, i.e.,

$$\dot{Q}_{e\text{-}p} = A\int_0^L dx P_{e\text{-}p}(x). \tag{6}$$

Here A is the cross section of the normal metal. In the normal case $P^N_{e\text{-}p}$ is independent of position, and thus $\dot{Q}^N_{e\text{-}p}=P^N_{e\text{-}p}\Omega$, where $\Omega=AL$ is the volume of the normal metal.

Proximity effect changes the electron-phonon heat current drastically. Most of the changes are limited within a thermal coherence length $\xi_T=\sqrt{\hbar D/(2\pi k_BT)}$ from the superconductors. This is illustrated in Fig. 3, which shows $P_{e\text{-}p}$ normalized to $P^N_{e\text{-}p}$ as a function of position and temperature. Note that changing T_e inside the normal metal does not affect the superconducting gap as the superconductors are assumed to be at the phonon temperature.

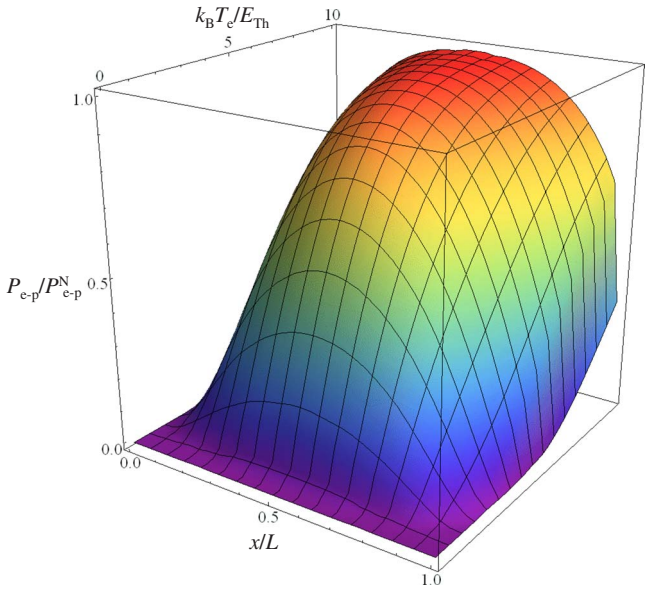

FIG. 3. (Color online) Position- and temperature-dependent heat current density $P_{e\text{-}p}$ between the electron and phonon systems inside the normal part of the SNS system of length L. Here $\phi=0$, $\Delta=20E_{Th}$, $T_p=0$, and the heat current density has been normalized to the normal-state value $P^N_{e\text{-}p}=\Sigma T_e^5$.

A relevant factor for the SNS system is the relation of the energy gap inside the superconductor to the Thouless energy of the weak link. This ratio is equal to the square of the ratio between the length of the junction and the superconducting coherence length. Figure 4 shows the position-averaged heat current as a function of electron temperature for different lengths of the junction. At low temperatures below the minigap, $k_BT \lesssim E_g$, the heat current is vanishingly small because

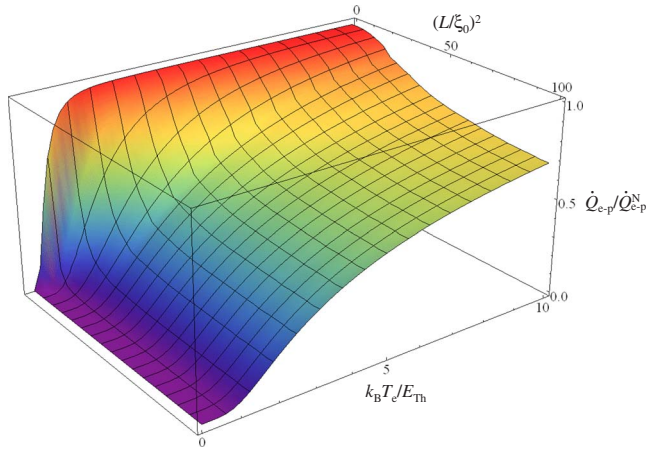

FIG. 4. (Color online) Dependence of the heat current on electron temperature and the length L of the junction compared to the zero-temperature coherence length $\xi_0=\sqrt{\hbar D/\Delta}$. Here $\phi=0$ and $T_p=0$.

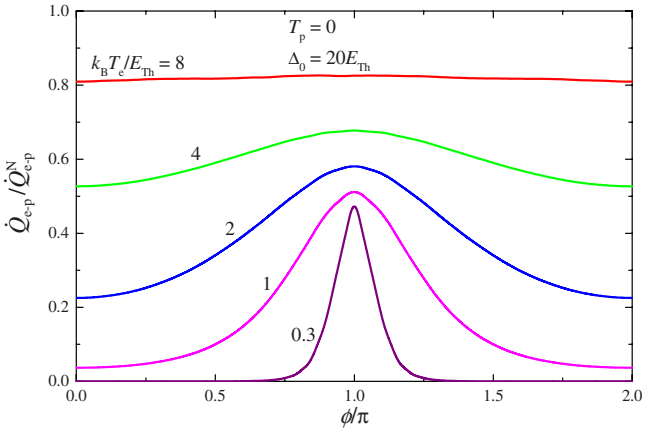

FIG. 5. (Color online) Phase-dependent electron-phonon heat current at a few different temperatures with $T_p=0$ and $\Delta=20E_{Th}$. The closing minigap for $\phi\rightarrow\pi$ shows up as a rapid increase in $\dot{Q}_{e\text{-}p}$ at low temperatures. For k_BT_e somewhat larger than the minigap, the phase dependence becomes much weaker although the overall heat current is still smaller than in the normal state.

of the lack of states inside the normal metal. However, also at higher temperatures there is some reduction, whose measurement is well within reach of state-of-the-art thermometry.

Apart from the temperature and length of the junction, the nature of the proximity effect is quite sensitive to the phase difference ϕ between the superconductors. This sensitivity is mainly due to the phase-dependent minigap in the density of states. This is illustrated in Fig. 5, where $\dot{Q}_{e\text{-}p}$ is plotted as a function of ϕ. The strongest dependence takes place naturally at temperatures close to the phase-dependent minigap. However, some phase dependence is still remaining even at higher temperatures.

In the long-junction regime $L\gg\xi_0$, $\phi=0$, and temperatures up to some $10E_T/k_B$, the temperature dependence of the power $\dot{Q}_{e\text{-}p}$ can be fitted rather well to a curve of the form

$$\dot{Q}_{e\text{-}p} = \dot{Q}^N_{e\text{-}p}\exp(-T^*/T), \tag{7}$$

where $T^*=cE_{Th}/k_B$ is a temperature scale describing the proximity-induced variations. For the prefactor we get $c\approx 3.5,\ldots,3.7$, depending on how large temperatures are included in the fit. This behavior resembles that of bulk superconductors,[15] but the gap Δ is replaced by T^*. However, in the SNS case the exponential behavior extends to comparatively larger temperatures than in bulk superconductors where one has to assume $k_BT\ll\Delta$ for the law to be valid.

As seen in Fig. 5, $\dot{Q}_{e\text{-}p}$ becomes independent of the phase at temperatures larger than the zero-phase minigap. In this case the temperature dependence can again be expressed with Eq. (7). However, for low temperatures the effective temperature scale becomes of the order of the phase-dependent minigap $E_g(\phi)$.

V. EXPERIMENTAL DETERMINATION

A possible experimental setup to measure the effects discussed above is shown in Fig. 6(a). The structure can be

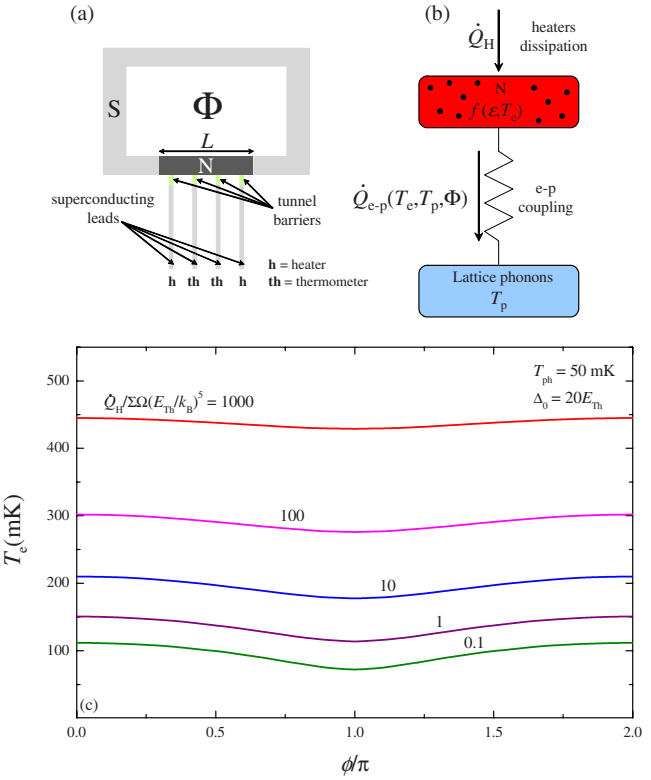

FIG. 6. (Color online) (a) Scheme of a possible experimental setup. A radio-frequency (rf) SQUID containing a SNS junction is threaded by a magnetic flux Φ which allows one to tune the electron-phonon interaction in the N region. Additional superconducting electrodes tunnel coupled to the N wire allow one to probe the averaged phase-dependent $\dot{Q}_{e\text{-}p}(T_e,T_p,\phi)$. These serve both as heaters (h) and thermometers (th). (b) Sketch of the thermal model of the N wire (see text). (c) Steady-state electron temperature inside the SNS junction as a function of the phase for a few driving powers at a phonon temperature $T_p=E_{Th}/(2k_B)$. For this curve, we chose $E_{Th}/k_B=100$ mK (see text).

fabricated through standard lithography techniques.[1] The device consists of a radio-frequency superconducting quantum interference device (SQUID),[16,17] where a superconducting loop is interrupted by a N wire of length L. The strength of the electron-phonon interaction in N can be modulated periodically by an externally applied magnetic field, which gives rise to a total flux Φ through the loop area. Neglecting the inductance of the superconducting loop, the phase difference then becomes $\phi=\Phi/(h/2e)$. The SQUID allows magnetoelectric characterization of the SNS junction, and thus also the determination of some of the relevant parameters of the N wire. For instance, the Thouless energy of the junction can be extracted from the temperature dependence of the SQUID critical supercurrent. Alternatively, the phase can be controlled by an externally driven current in the case when the superconductors are not connected. However, in these cases only phases $\phi\approx-\pi/2,\ldots,\pi/2$ can be accessed. The N region is connected to four additional superconducting electrodes through oxide barriers, so to realize normal-metal-insulator-superconductor (NIS) tunnel junctions. The NIS junctions are used to heat (or eventually to cool) the electrons in N and as sensitive thermometers to measure T_e.[1]

Both the NS contacts and the NIS junctions provide nearly ideal thermal isolation of the N region, and therefore in the following we neglect the thermal conductance through the superconductors. One further advantage of using tunnel junctions directly connected to N stems from the fact that the state of the electron system and the superconducting correlations induced by proximity from S electrodes will be virtually unaffected by the presence of tunnel-coupled probes.[18] The basic requirements for this are that the currents driven through the NIS junctions are much smaller than the SNS critical current and that the tunnel junction resistances are much larger than the resistance of the normal metal. These requirements are easy to satisfy in practice.

Figure 6(b) shows a sketch of the relevant thermal model of the wire in the proposed setup.[15] Upon heating electrons with a constant power $\dot{Q}_H$ provided by the NIS heaters the steady-state T_e established in N will depend on the energy relaxation mechanisms occurring in the wire. In metals at low lattice temperature (typically below 1 K), the main relaxation mechanism is related to electron-phonon interaction which in the present setup is strongly phase dependent. In practice, what will be measured is the power flowing between the electron and phonon systems averaged over the wire volume Ω, i.e., $\dot{Q}_{\text{e-p}}(T_e, T_p, \phi)$. At fixed lattice temperature the predicted steady-state phase-dependent T_e thus follows from the solution of the thermal-balance equation

$$\dot{Q}_H + \dot{Q}_{\text{e-p}}(T_e, T_p, \phi) = 0. \tag{8}$$

The resulting electron temperature T_e can then be probed with the NIS thermometers.

The result of such a heat balance is plotted in Fig. 6(c) which displays the steady-state electron temperature T_e for some values of $\dot{Q}_H$ as the phase is varied and the bath temperature is $T_p = 50$ mK. To illustrate the strength of the effect, we chose a typical $E_{\text{Th}}/k_B = 100$ mK. For each $\dot{Q}_H$ the electronic temperature is strongly modulated by the phase, and it decreases by an increasing ϕ due to the enhancement of the electron-phonon interaction for phase difference close to π (see Fig. 5). In particular, for $\dot{Q}_H = 0.1\Sigma\Omega(E_{\text{Th}}/k_B)^5$, variation in T_e of the order of 40 mK ($0.4E_{\text{Th}}$) can be achieved by varying the phase (flux), while even for the large injected power $\dot{Q}_H = 100\Sigma\Omega(E_{\text{Th}}/k_B)^5$ the variation amplitude is somewhat below 30 mK ($0.3E_{\text{Th}}$).

Let us discuss some of the typical material parameters for the proposed measurement. By choosing, for instance, aluminum (Al) as S material (with $\Delta_0 = 200$ μeV), copper (Cu) as N wire (with $D = 0.01$ m^2 s^{-1} and $\Sigma = 2 \times 10^9$ Wm^{-3} K^{-5}, see Ref. 1), and length $L = 0.8$ μm, we get $\Delta_0/E_T = 19$ and $E_{\text{Th}}/k_B = 10$ μeV $= 120$ mK. Moreover, if we assume that the wire is 50 nm thick and 400 nm wide, the "unit power" in Fig. 6 is $\Sigma\Omega(E_{\text{Th}}/k_B)^5 = 0.8$ fW.

VI. CONCLUSIONS

In bulk superconductors, the presence of the energy gap leads to a strong suppression of the heat transport between the electron and phonon systems.[15] In this paper we show that a similar effect can be expected for normal metals in close proximity to the superconductors and suggest how it can be probed. Additionally, the heat current between the two systems can be controlled *in situ* by changing the phase difference between two superconducting contacts. The suppression of the heat conductance is especially relevant in thermal radiation detectors—for example in the proximity Josephson sensor (PJS) suggested in Ref. 2. This is because of two factors. First, the weaker the thermal relaxation, the stronger is the temperature rise for a given power of radiation. Second, the main cause of noise in these devices is related to the strongest thermal relaxation channel, which typically is the electron-phonon coupling. Reducing this coupling will therefore also reduce the noise. Both of these factors will improve the sensitivity of such thermal detectors.

ACKNOWLEDGMENTS

We thank Pauli Virtanen for discussions and help with the numerics. T.T.H. was supported by the Academy of Finland, and F.G. was partially supported by the NanoSciERA "NanoFridge" project of the EU. T.T.H. acknowledges the hospitality of the Kavli Institute of Nanotechnology at the Delft University of Technology, where part of this work was carried out.

APPENDIX

The self-energy for the electron-phonon scattering in the case of thermal phonons at temperature T_p and with the general Keldysh Green's function for the electrons is given by[8]

$$\check{\Sigma}_{\text{e-p}} = \begin{pmatrix} \hat{\Sigma}^R & \hat{\Sigma}^K \\ 0 & \hat{\Sigma}^A \end{pmatrix},$$

where

$$\hat{\Sigma}^K = \lambda \int \frac{d\omega}{4} \omega^2 \,\text{sgn}(\omega) \left[\coth\left(\frac{\omega}{2k_B T_p}\right) \hat{g}^K(\epsilon+\omega) - \hat{A}(\epsilon+\omega) \right],$$

$$\hat{\Sigma}^{R/A} = \lambda \int \frac{d\omega}{4} \omega^2 \,\text{sgn}(\omega) \left[\coth\left(\frac{\omega}{2k_B T_p}\right) \hat{g}^{R/A}(\epsilon+\omega) \mp \frac{1}{2} \hat{g}^K(\epsilon+\omega) \right].$$

Here $\hat{A} = \hat{g}^R - \hat{g}^A$ is the spectral function and $\hat{g}^{R,A,K}$ are the retarded, advanced, and the Keldysh Green's functions, respectively. From these self-energies, the collision integral appearing in Usadel equation is

$$\check{I}_{\text{e-p}} = \begin{pmatrix} \hat{I}^R & \hat{I}^K \\ 0 & \hat{I}^A \end{pmatrix} = [\check{g}, \check{\Sigma}_{\text{e-p}}].$$

We are mostly interested in the Keldysh part, which has two components: $I_L = \text{Tr}[\hat{I}^K]/2$ and $I_T = \text{Tr}[\hat{\tau}_3 \hat{I}^K]/2$. In the following we parametrize the Green's function by $\hat{g}^K = \hat{g}^R \hat{h} - \hat{h} \hat{g}^A$, $\hat{h} = f_L \hat{\tau}_0 + f_T \hat{\tau}_3$, and

$$\hat{g}^R = \begin{pmatrix} g & fe^{i\phi} \\ -fe^{-i\phi} & -g \end{pmatrix}.$$

Moreover, the normalization condition implies $g^2 - f^2 = 1$. The advanced Green's function can then be obtained by $\hat{g}^A = -\hat{\tau}_3(\hat{g}^R)^\dagger\hat{\tau}_3$. Note that inside a proximity structure, all the three variables, g, f, and ϕ, are in general complex valued. Moreover, we define $N = \mathrm{Re}[g]$ (local density of states) and the real quantities

$$F_c = \mathrm{Re}[f\cos(\phi)], \quad F_s = \mathrm{Re}[f\sin(\phi)],$$

$$\tilde{F}_c = \mathrm{Im}[f\cos(\phi)], \quad \tilde{F}_s = \mathrm{Im}[f\sin(\phi)]. \tag{A1}$$

After some lengthy but straightforward algebra, the collision integrals become

$$I_T = \lambda\int d\omega\omega^2\,\mathrm{sgn}(\omega)\Big\{[F_c(\epsilon+\omega)\tilde{F}_s(\epsilon) - F_s(\epsilon+\omega)\tilde{F}_c(\epsilon)] \times\left[\coth\left(\frac{\omega}{2k_BT_p}\right)f_L(\epsilon+\omega) - 1\right] + [F_s(\epsilon)\tilde{F}_c(\epsilon+\omega) - F_c(\epsilon)\tilde{F}_s(\epsilon+\omega)]\coth\left(\frac{\omega}{2k_BT_p}\right)f_L(\epsilon) + [N(\epsilon)N(\epsilon+\omega) + \tilde{F}_c(\epsilon+\omega)\tilde{F}_c(\epsilon) + \tilde{F}_s(\epsilon+\omega)\tilde{F}_s(\epsilon)]\coth\left(\frac{\omega}{2k_BT_p}\right) \times[f_T(\epsilon+\omega) - f_T(\epsilon)] + N(\epsilon)N(\epsilon+\omega)[f_L(\epsilon)f_T(\epsilon+\omega) + f_L(\epsilon+\omega)f_T(\epsilon)]\Big\} \tag{A2}$$

and

$$I_L = \lambda\int d\omega\omega^2\,\mathrm{sgn}(\omega)\Big\{[N(\epsilon)N(\epsilon+\omega) - F_c(\epsilon)F_c(\epsilon+\omega) - F_s(\epsilon)F_s(\epsilon+\omega)]\Big\{\coth\left(\frac{\omega}{2k_BT_p}\right)[f_L(\epsilon+\omega) - f_L(\epsilon)] - 1 + f_L(\epsilon)f_L(\epsilon+\omega)\Big\} + [F_s(\epsilon)\tilde{F}_c(\epsilon+\omega) - F_c(\epsilon)\tilde{F}_s(\epsilon+\omega)] \times\left[f_L(\epsilon) + \coth\left(\frac{\omega}{2k_BT_p}\right)\right]f_T(\epsilon+\omega) + [F_s(\epsilon+\omega)\tilde{F}_c(\epsilon) - F_c(\epsilon+\omega)\tilde{F}_s(\epsilon)]\left[f_L(\epsilon+\omega) - \coth\left(\frac{\omega}{2k_BT_p}\right)\right]f_T(\epsilon) + [N(\epsilon)N(\epsilon+\omega) - \tilde{F}_c(\epsilon)\tilde{F}_c(\epsilon+\omega) - \tilde{F}_s(\epsilon)\tilde{F}_s(\epsilon+\omega)]f_T(\epsilon) \times f_T(\epsilon+\omega)\Big\}. \tag{A3}$$

These simplify considerably in the quasiequilibrium limit where $f_T = 0$ and $f_L = \tanh[\epsilon/(2k_BT)]$. In that case one obtains the collision integral presented in Eq. (1).

*tero.heikkila@tkk.fi

[1] F. Giazotto, T. T. Heikkilä, A. Luukanen, A. M. Savin, and J. P. Pekola, Rev. Mod. Phys. **78**, 217 (2006).

[2] F. Giazotto, T. T. Heikkilä, G. Pepe, P. Helistö, A. Luukanen, and J. P. Pekola, Appl. Phys. Lett. **92**, 162507 (2008).

[3] P. G. de Gennes and D. Saint-James, Phys. Lett. **4**, 151 (1963).

[4] P. Virtanen and T. T. Heikkilä, Appl. Phys. A: Mater. Sci. Process. **89**, 625 (2007).

[5] H. le Sueur, P. Joyez, H. Pothier, C. Urbina, and D. Esteve, Phys. Rev. Lett. **100**, 197002 (2008).

[6] F. Zhou, P. Charlat, B. Spivak, and B. Pannetier, J. Low Temp. Phys. **110**, 841 (1998).

[7] K. D. Usadel, Phys. Rev. Lett. **25**, 507 (1970).

[8] N. B. Kopnin, *Theory of Nonequilibrium Superconductivity* (Clarendon, Oxford, 2001).

[9] A. Schmid and G. Schön, J. Low Temp. Phys. **20**, 207 (1975).

[10] J. C. Hammer, J. C. Cuevas, F. S. Bergeret, and W. Belzig, Phys. Rev. B **76**, 064514 (2007).

[11] In order to find the kernel $K(\epsilon,\omega)$, we parametrize Eq. (2) with the Riccati-type parametrization detailed for example in Ref. 10. This parametrization, contrary to the often employed θ parametrization (see, e.g., Ref. 4), can access all values of the phase difference ϕ between the superconductors.

[12] S. B. Kaplan, C. C. Chi, D. N. Langenberg, J. J. Chang, S. Jafarey, and D. J. Scalapino, Phys. Rev. B **14**, 4854 (1976).

[13] J. Rammer, *Quantum Transport Theory* (Perseus Books, Reading, MA, 1998).

[14] F. C. Wellstood, C. Urbina, and J. Clarke, Phys. Rev. B **49**, 5942 (1994).

[15] A. V. Timofeev, C. P. García, N. B. Kopnin, A. M. Savin, M. Meschke, F. Giazotto, and J. P. Pekola, Phys. Rev. Lett. **102**, 017003 (2009).

[16] J. J. A. Baselmans, B. J. van Wees, and T. M. Klapwijk, Appl. Phys. Lett. **79**, 2940 (2001).

[17] L. Angers, F. Chiodi, G. Montambaux, M. Ferrier, S. Guéron, H. Bouchiat, and J. C. Cuevas, Phys. Rev. B **77**, 165408 (2008).

[18] F. Giazotto, T. T. Heikkilä, F. Taddei, R. Fazio, J. P. Pekola, and F. Beltram, J. Low Temp. Phys. **136**, 435 (2004).